# Effects of ATP, $Mg^{2+}$, and redox agents on the $Ca^{2+}$ dependence of RyR channels from rat brain cortex

**Ricardo Bull,[1,4] José Pablo Finkelstein,[4] Alexis Humeres,[4] María Isabel Behrens,[2,4] and Cecilia Hidalgo[3,4]**

[4]*Centro Fondo de Investigación Avanzada en Areas Prioritarias (FONDAP) de Estudios Moleculares de la Célula, Facultad de Medicina, Universidad de Chile;* [1]*Programa de Fisiología y Biofísica, Instituto de Ciencias Biomédicas, Facultad de Medicina, Universidad de Chile;* [2]*Departamento de Neurología y Neurocirugía, Hospital Clínico, Universidad de Chile; and* [3]*Programa de Biología Celular y Molecular, Instituto de Ciencias Biomédicas, Facultad de Medicina, Universidad de Chile, Santiago, Chile*

**Bull R, Finkelstein JP, Humeres A, Behrens MI, Hidalgo C.** Effects of ATP, $Mg^{2+}$, and redox agents on the $Ca^{2+}$ dependence of RyR channels from rat brain cortex. *Am J Physiol Cell Physiol* 293: C162–C171, 2007. First published March 14, 2007; doi:10.1152/ajpcell.00518.2006.—Despite their relevance for neuronal $Ca^{2+}$-induced $Ca^{2+}$ release (CICR), activation by $Ca^{2+}$ of ryanodine receptor (RyR) channels of brain endoplasmic reticulum at the [ATP], [$Mg^{2+}$], and redox conditions present in neurons has not been reported. Here, we studied the effects of varying *cis*-(cytoplasmic) free ATP concentration ([ATP]), [$Mg^{2+}$], and RyR redox state on the $Ca^{2+}$ dependence of endoplasmic reticulum RyR channels from rat brain cortex. At pCa 4.9 and 0.5 mM adenylylimidodiphosphate (AMP-PNP), increasing free [$Mg^{2+}$] up to 1 mM inhibited vesicular [$^3$H]ryanodine binding; incubation with thimerosal or dithiothreitol decreased or enhanced $Mg^{2+}$ inhibition, respectively. Single RyR channels incorporated into lipid bilayers displayed three different $Ca^{2+}$ dependencies, defined by low, moderate, or high maximal fractional open time ($P_o$), that depend on RyR redox state, as we have previously reported. In all cases, *cis*-ATP addition (3 mM) decreased threshold [$Ca^{2+}$] for activation, increased maximal $P_o$, and shifted channel inhibition to higher [$Ca^{2+}$]. Conversely, at pCa 4.5 and 3 mM ATP, increasing *cis*-[$Mg^{2+}$] up to 1 mM inhibited low activity channels more than moderate activity channels but barely modified high activity channels. Addition of 0.5 mM free [ATP] plus 0.8 mM free [$Mg^{2+}$] induced a right shift in $Ca^{2+}$ dependence for all channels so that [$Ca^{2+}$] $<30$ $\mu$M activated only high activity channels. These results strongly suggest that channel redox state determines RyR activation by $Ca^{2+}$ at physiological [ATP] and [$Mg^{2+}$]. If RyR behave similarly in living neurons, cellular redox state should affect RyR-mediated CICR.

$Ca^{2+}$-induced $Ca^{2+}$ release; $Ca^{2+}$ release channels; endoplasmic reticulum; thimerosal; 2,4-dithiothreitol; ryanodine receptor

TRANSIENT ELEVATIONS OF cytoplasmic $Ca^{2+}$ concentration ([$Ca^{2+}$]) have a central role in several key neuronal functions such as excitability, synaptic transmission, synaptic plasticity, and gene expression (3, 4, 56). In this context, a role for $Ca^{2+}$ release from intracellular stores as an amplification mechanism of $Ca^{2+}$ signals is emerging (5, 12, 23, 52, 61–63). In particular, recent studies indicate that $Ca^{2+}$ release mediated by ryanodine receptors (RyR) participates in neuronal synaptic plasticity and gene expression (3, 4, 10, 11, 22). Activation of RyR-mediated $Ca^{2+}$ release in neurons may take place via $Ca^{2+}$-induced $Ca^{2+}$ release (CICR) (3–5, 26, 52, 61, 62) or through depolarization-induced $Ca^{2+}$ release (18, 50), the two physiological mechanisms displayed by cardiac or skeletal muscle, respectively. Presynaptic CICR has been implicated in many different types of synapses (5). Additionally, RyR-mediated CICR following activation of *N*-methyl-D-aspartate (NMDA) receptors is required to elicit $Ca^{2+}$ signals in hippocampal postsynaptic dendritic spines (19), albeit opposing results have also been reported (32).

RyR channels are activated by several cytoplasmic agonists/modulators such as $Ca^{2+}$ and ATP (44, 70). This information comes mostly from studies performed in RyR channels from skeletal or cardiac muscle (17, 21). Despite the emerging importance of RyR-mediated $Ca^{2+}$ release for brain function, the properties and regulation of RyR channels from brain have been less studied than those of their skeletal or cardiac counterparts. There are a few reports describing their activity either measured at the single-channel level (2, 8, 34, 38, 39, 43, 55) or as [$^3$H]ryanodine binding density, taking advantage of the fact that ryanodine binds preferentially to RyR channels in the open state (42, 51, 57, 69).

Studies on microsomal fractions isolated from different rat brain regions, such as cerebral cortex, cerebellum, hippocampus, and brainstem, have shown that all fractions exhibit [$^3$H]ryanodine binding, albeit the microsomes isolated from cerebral cortex exhibit the highest density of ryanodine binding sites (69). The binding of [$^3$H]ryanodine to brain microsomes is activated by $Ca^{2+}$ in the micromolar range and inhibited by both $Ca^{2+}$ and $Mg^{2+}$ at millimolar concentrations and by micromolar Ruthenium red (42, 57, 69). In addition, ATP (or nonhydrolyzable ATP analogs) and caffeine also enhance [$^3$H]ryanodine binding (42, 51, 57, 69).

Murine brain expresses the three mammalian RyR isoforms, albeit RyR2 is enriched in most brain regions (24, 33); in particular, bovine and rabbit brain cortex express only RyR2 and RyR3 (24, 49). Yet, we have reported that the response to *cis*-[$Ca^{2+}$] displayed by single RyR channels from rat brain cortex differs markedly from the $Ca^{2+}$ responses of single RyR2 channels from cardiac muscle (38, 39) or of RyR3 channels from bovine or rabbit diaphragm muscle (28, 47, 58). Thus, after fusion with planar lipid bilayers, single RyR channels from endoplasmic reticulum (ER) isolated from rat brain display three different $Ca^{2+}$ dependencies, characterized by low, moderate, or high maximal fractional open time ($P_o$) (8,

Address for reprint requests and other correspondence: R. Bull, ICBM, Facultad de Medicina, Universidad de Chile, Casilla 70005, Santiago 7, Chile (e-mail: rbull@med.uchile.cl).

38, 39). In comparison, single RyR2 channels from cardiac muscle display only the two $Ca^{2+}$ dependencies characterized by moderate or high maximal $P_o$ (39). Likewise, single RyR3 channels from skeletal muscle only display one $Ca^{2+}$ dependence, characterized by high maximal $P_o$ (28, 47, 58). Furthermore, at micromolar [$Ca^{2+}$], RyR channels from rat brain cortex ER display most frequently low activity instead of the high activity most frequently observed both in cardiac RyR2 (14, 16, 36, 38, 39, 54) and skeletal RyR3 (28, 47, 58). Thus RyR channels from rat brain cortex ER are usually very poorly activated by 10 μM cytoplasmic $Ca^{2+}$, whereas cardiac RyR2 (14, 16, 36, 38, 39) and skeletal RyR3 (28, 47) channels are fully activated by this [$Ca^{2+}$].

In our previous studies, we determined brain cortex RyR single-channel response to varying *cis*-[$Ca^{2+}$] in the absence of other RyR physiological modulators. This is an important factor to consider, since, despite the emerging importance of RyR-mediated CICR for brain function (5, 12, 23, 52, 61, 62), it is not known how $Ca^{2+}$ activates these channels at the concentrations of $Mg^{2+}$ and ATP present in neurons in physiological conditions. In addition, RyR channels are very sensitive to redox modification, as detailed below. Changes in RyR redox state affect activity of RyR channels from all sources, including brain, and modify their calcium dependence in particular. We have reported that, through sequential modification of its redox state directly in the bilayer, the same single RyR channel can display the three $Ca^{2+}$ responses observed in RyR from brain cortex (39). In brief, highly reduced RyR channels from rat brain cortex ER respond poorly to $Ca^{2+}$ activation and reach maximal $P_o$ values $<0.1$; on account of this behavior, we named them low $P_o$ channels. Oxidation in the bilayer activates these channels by increasing $P_o$ at micromolar [$Ca^{2+}$] and decreasing the inhibition observed at millimolar [$Ca^{2+}$], yielding sequentially and in stepwise fashion first the moderate and then the high $P_o$ behavior. These modifications are reversible, since reducing agents reverse all these changes (39). These observations strongly suggest that these three $Ca^{2+}$ dependencies arise from three different discrete redox states of the same RyR channel isoform. In addition to their differential behavior toward $Ca^{2+}$, we have found that ATP also differentially activates RyR channels depending on their redox state; lower ATP concentrations are required to attain maximal activation in oxidized than in reduced channels (8).

As a first approximation to further characterize the RyR channels of brain cortex ER vesicles, in the present study we investigated the effect of ATP on the response to cytoplasmic [$Ca^{2+}$] of single RyR channels incorporated in lipid bilayers. In addition, we studied both at the single-channel level and through [$^3$H]ryanodine binding the inhibition by $Mg^{2+}$ on the activity of RyR channels maximally activated by ATP and $Ca^{2+}$. Finally, we measured the $Ca^{2+}$ dependence of single channels at near physiological uncomplexed (from now on designated as free) concentrations of $Mg^{2+}$ and ATP. We found that incubation with the sulfhydryl (SH) reducing agent 2,4-dithiothreitol (DTT) enhanced, while the SH alkylating agent thimerosal decreased, the inhibitory effect of $Mg^{2+}$ on [$^3$H]ryanodine binding. We also found that, at near physiological free concentrations of ATP and $Mg^{2+}$ (0.5 and 0.8 mM, respectively), single RyR channel activation by $Ca^{2+}$ required higher [$Ca^{2+}$] than in the absence of ATP and $Mg^{2+}$; this behavior was observed in all RyR channels regardless of their $Ca^{2+}$ dependence. We discuss possible implications of these findings for RyR-mediated CICR in living neurons.

## MATERIALS AND METHODS

*Isolation of membrane fractions.* RyR-enriched ER vesicles were obtained from brain cortex (excluding the hippocampus) of 12-wk-old Sprague-Dawley rats, as previously described (38); 5 mM DTT was used in all steps of the isolation procedure. Small aliquots were quickly frozen in liquid $N_2$ and stored at −80°C. The experimental protocol complied with the "Guiding Principles for Research Involving Animals and Human Beings" of the American Physiological Society and was approved by the Bioethics Committee for Investigation in Animals of the Facultad de Medicina, Universidad de Chile.

*[$^3$H]ryanodine binding.* To measure equilibrium [$^3$H]ryanodine binding, vesicles (0.1 mg/ml) were incubated in high ionic strength [500 mM KCl, 0.5 mM adenylylimidodiphosphate (AMP-PNP), 20 mM MOPS-Tris, pH 7.0] solutions containing the ATP analog 5′-AMP-PNP and varying free [$Mg^{2+}$]. After incubation of vesicles with 10 nM [$^3$H]ryanodine for 120 min at 37°C, total binding density was determined by filtration as described (9). Nonspecific binding was determined in the additional presence of 10 μM ryanodine. Free [$Ca^{2+}$] and [$Mg^{2+}$] were calculated with the WinMAXC program (**http://www.stanford.edu/~cpatton/wmaxc.zip**), using the constants provided in file CMC0204E.TCM. The constants for AMP-PNP were calculated according to values given elsewhere (67). To test the effects of the redox agents DTT and thimerosal on [$^3$H]ryanodine binding, vesicles were preincubated for 5 min with 10 mM DTT or 0.5 mM thimerosal at room temperature. In the case of incubation with DTT, 10 mM DTT was also added during the binding assay. After incubation with thimerosal, the concentration of thimerosal decreased to 17 μM following dilution of vesicles in the binding assay solutions.

*Channel recording and analysis.* Planar phospholipid bilayers were painted, and ER vesicles were added to the *cis*-(cytoplasmic) compartment as previously described (38). After fusion of ER vesicles to the lipid bilayer, the *cis*-compartment was perfused with seven times the compartment volume of a solution containing 225 mM HEPES-Tris, pH 7.4. The *trans*-(intrareticular) compartment was replaced with 40 mM $Ca^{2+}$-HEPES and 15 mM Tris-HEPES, pH 7.4. The charge carrier was $Ca^{2+}$ in all experiments. To set the desired *cis*-free [$Ca^{2+}$], HEDTA and/or EGTA was added to the *cis*-compartment. The total concentrations of HEDTA and/or EGTA, ATP, $Ca^{2+}$, and $Mg^{2+}$ required for each free [$Ca^{2+}$], [$Mg^{2+}$], and [ATP] were calculated with the WinMAXC program. In experiments with ATP and $Mg^{2+}$, the total [ATP] was 5 mM or greater. To promote SH modification of the channel in the bilayer, 10–20 μM thimerosal was added to the cytoplasmic compartment; when a stepwise change in $P_o$ was observed (30–200 s), the reaction was stopped by removal of the nonreacted reagent through extensive perfusion of the *cis*-compartment (7–14 times the compartment volume) with a solution containing 225 mM HEPES-Tris, pH 7.4. All experiments were carried out at room temperature (22–24°C). Voltage was applied to the *cis*-compartment, and the *trans*-compartment was held at virtual ground through an operational amplifier in a current-to-voltage configuration. Current signals were both recorded on tape and acquired online.

Data were filtered at 400 Hz (−3 dB) using an eight-pole low-pass Bessel type filter (902 LPF; Frequency Devices, Haverhill, MA) and digitized at 2 kHz with a 12-bit analog-to-digital (A/D) converter (Labmaster DMA interface; Scientific Solutions, Solon, OH) using Axotape software (Axon Instruments, Burlingame, CA). $P_o$ was computed from recordings of 30 s or longer using pClamp software (Axon Instruments). $P_o$ was calculated as $P_o^*$, dividing the mean current of the channel recording by single-channel current amplitude, as described previously (8). Briefly, current amplitude was measured in long-lasting fully open events. Low and moderate $P_o$ channels in the presence of [Ca] >10 μM gated with fast kinetics between the closed

and open states, suggestive of substates, as previously reported (8); however, the recordings showed long-lasting openings (>30 ms), especially in the presence of ATP, that allowed measurements of channel currents.

*Data expression and curve analysis.* Data are expressed as mean values ± SE. $Ca^{2+}$ dependence of single-channel $P_o^*$ values was fitted with the following general function (29)

$$P_o^* = \{(P_{o\,max} \times [Ca^{2+}]^n)/([Ca^{2+}]^n + K_a^n)\} \times \{K_i/([Ca^{2+}] + K_i)\} \quad (1)$$

*Equation 1* gives $P_o^*$ values as a function of *cis*-$[Ca^{2+}]$. $P_{o\,max}$ corresponds to the theoretical $P_o$ value of maximal activation by $Ca^{2+}$. $K_a$ and $K_i$ correspond to the $Ca^{2+}$ concentrations for half-maximal activation and inhibition, respectively, of channel activity, and $n$ is the Hill coefficient for $Ca^{2+}$ activation.

For low $P_o$ channels, both in the absence of ATP and at near physiological [ATP] and $[Mg^{2+}]$, $P_{o\,max}$ was fixed at 0.65, since this was the $P_{o\,max}$ value obtained for low $P_o$ channels at 3 mM ATP. For moderate and high $P_o$ channels, $P_{o\,max}$ was fixed to 1.0, since they were fully activated in the presence of 3 mM ATP.

Magnesium inhibition data were fitted with the following equation

$$Z = Z_{in}/\{([Mg^{2+}]/K_{i\,Mg})^n + 1\} \quad (2)$$

In *Eq. 2*, Z yields B or $P_o^*$ obtained in binding or single-channel experiments, respectively. $Z_{in}$ corresponds to B or $P_o^*$ values obtained in the absence of $Mg^{2+}$, $K_{i\,Mg}$ is the concentration of $Mg^{2+}$ for half-maximal inhibition, and $n$ is the Hill coefficient for $Mg^{2+}$ inhibition. In binding experiments, $n$ was fixed to 1.0.

Nonlinear fitting was performed with the SigmaPlot software (Systat Software, Richmond, CA). To include variability of experimental data in the parameter values, curve fitting was performed using all individual values for each condition studied. All parameter values obtained differed significantly from zero ($P < 0.015$, Student's $t$-test). Comparison of the differences among parameter values obtained in different conditions was statistically analyzed using Student's $t$-test with the Welch correction.

*Materials.* Lipids were obtained from Avanti Polar Lipids (Birmingham, AL). All reagents used were of analytical grade. Ryanodine, bovine serum albumin, thimerosal, AMP-PNP, and protease inhibitors (leupeptin, pepstatin A, benzamidine, and phenylmethylsulfonyl fluoride) were from Sigma Chemical (St. Louis, MO). DTT was from Calbiochem (La Jolla, CA), and [$^3$H]ryanodine was from NEN Life Sciences (Boston, MA).

## RESULTS

In this work, we determined the effects of $Mg^{2+}$ and ATP on the $Ca^{2+}$ dependence of RyR channels from rat brain cortex ER, which had different redox states. RyR activity was evaluated with two different experimental approaches: by measuring [$^3$H]ryanodine binding to the population of RyR channels present in ER vesicles or by determining RyR single-channel activity.

*Effect of $Mg^{2+}$ on [$^3$H]ryanodine binding.* We investigated the effect of $Mg^{2+}$ on [$^3$H]ryanodine binding at a constant $[Ca^{2+}]$ of 13 ± 2 μM in the presence of 0.5 mM AMP-PNP. This $[Ca^{2+}]$ was selected because maximal [$^3$H]ryanodine binding to rat brain cortical vesicles has been reported at this $[Ca^{2+}]$ (69). In the different vesicle preparations, [$^3$H]ryanodine binding density was in the range of 0.37–0.88 pmol/mg. To compare the results obtained with different preparations, binding was normalized against the value determined in the absence of $Mg^{2+}$. Increasing free $[Mg^{2+}]$ up to 1 mM produced a significant inhibition ($P < 0.001$) of [$^3$H]ryanodine binding to control ER vesicles (not incubated with redox-modifying agents) (Fig. 1), with a $K_{i\,Mg}$ value given by the fit of 0.85 ± 0.15 mM (parameter value ± SE). Incubation with the SH alkylating agent thimerosal decreased the inhibitory effect of $Mg^{2+}$ compared with control vesicles, increasing the $K_{i\,Mg}$ value to 2.9 ± 0.8 mM ($P = 0.024$); in contrast, incubation with the reducing agent DTT enhanced the inhibitory effect of $Mg^{2+}$ on [$^3$H]ryanodine binding, reducing $K_{i\,Mg}$ to 0.48 ± 0.07 mM ($P = 0.031$; Fig. 1).

*Single-channel experiments.* Single RyR channel recordings were obtained after fusion of the ER vesicle preparation from rat brain cortex with planar lipid bilayers. In this work, channels recorded in the bilayer as isolated (not incubated with SH-modifying agents) will be called control channels. Additionally, channels were classified into low, moderate, and high $P_o$ channels according to their extent of activation by cytoplasmic $[Ca^{2+}]$ (in the absence of other agonists or inhibitors), as previously described (8, 38). Of all control channels studied (before any redox modification) ($N = 77$), 77% displayed the low $P_o$ behavior, 22% showed the moderate $P_o$ behavior, and only 1% showed the high $P_o$ behavior.

*Effect of ATP on RyR $Ca^{2+}$ dependence.* As detailed in MATERIALS AND METHODS, we will use $P_o^*$ whenever we describe the experimental values of channel fractional open time and $P_o$ to describe in general fractional open time. In a previous report, we showed that activation of RyR channels by ATP at fixed 0.1 or 10 μM $[Ca^{2+}]$ induced activation of channels with the low, moderate, or high $P_o$ response to $Ca^{2+}$ (8). Here we investigated the response of single channels to varying *cis*-$Ca^{2+}$ concentrations at a fixed free [ATP] of 3 mM. This concentration was selected because, at this [ATP], all channels have attained maximal activation by ATP (8), and thus it is possible to obtain the most marked changes in $Ca^{2+}$ dependence for low, moderate, and high $P_o$ channels. Representative channels displaying the low, moderate, or high $P_o$ behaviors, determined in the absence or presence of ATP, are shown in Fig. 2. Figure 2, *left*, shows the typical three responses to $Ca^{2+}$ of brain RyR

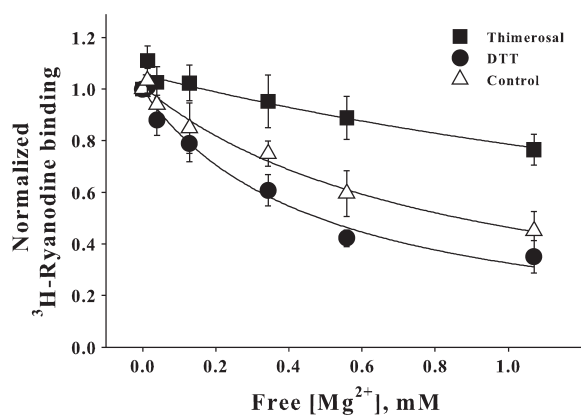


Fig. 1. $Mg^{2+}$ inhibition of specific [$^3$H]ryanodine binding to rat brain cortex endoplasmic reticulum (ER) vesicles. Data were obtained from binding experiments at 13 ± 2 μM free $Ca^{2+}$ concentration ($[Ca^{2+}]$) to control (triangles, $N = 4$), thimerosal-modified (squares, $N = 4$), or DTT-exposed (circles, $N = 5$) vesicles. Symbols and error bars depict mean ± SE values, respectively. Data are shown normalized because of the dispersion of the binding values obtained with the different preparations in the absence of $Mg^{2+}$, both in control and preincubated vesicles. The absolute values (mean ± SE) for DTT- or thimerosal-incubated vesicles were 0.32 ± 0.05 pmol/mg ($N = 5$) and 0.41 ± 0.09 pmol/mg ($N = 4$), respectively. For comparison, those of control vesicles were 0.59 ± 0.11 pmol/mg ($N = 4$). The solid lines show the best nonlinear fits to *Eq. 2* of all individual experimental data values obtained in the 3 different redox conditions (see MATERIALS AND METHODS). Fitted parameters are given in RESULTS.

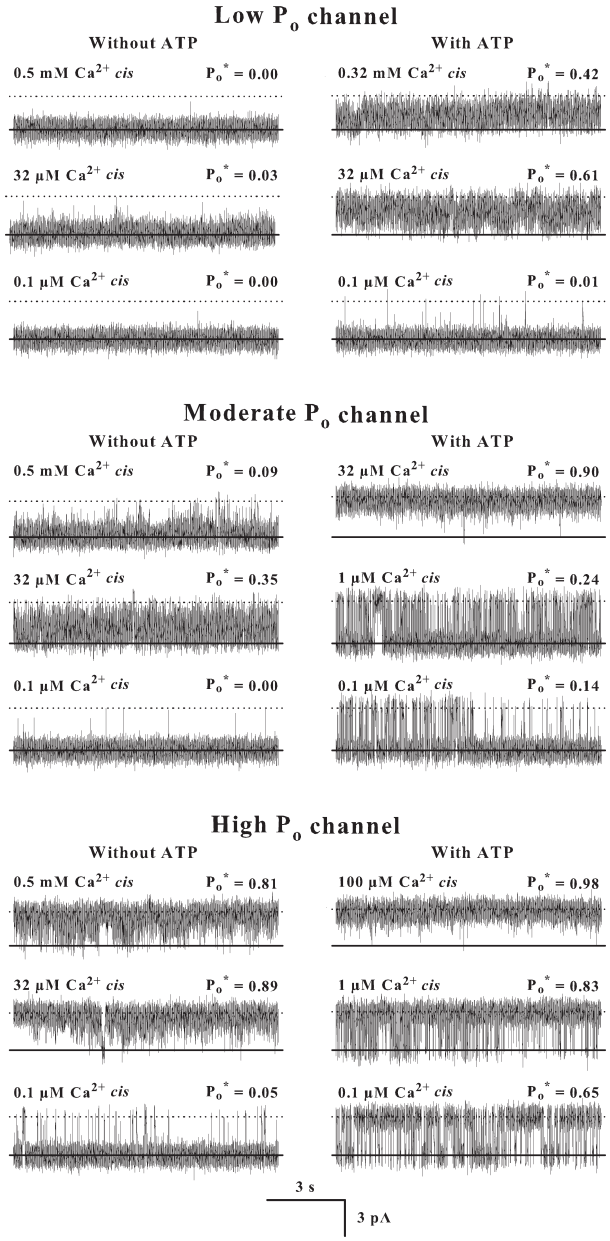


Fig. 2. The effect of ATP on $Ca^{2+}$ activation of single brain ryanodine receptor (RyR) channels with low, moderate, or high fractional open time ($P_o$) behavior. Representative current recordings were obtained without (*left*) or with ATP (*right*) at the indicated cytoplasmic free [$Ca^{2+}$]. ATP was added to the cytoplasmic compartment of a single control channel that displayed low $P_o$ (*top*) or moderate $P_o$ $Ca^{2+}$ dependence (*middle*) and to a channel that, after incubation with thimerosal, attained the high $P_o$ behavior (*bottom*). Average $P_o^*$ values, calculated from at least 120 s of continuous recordings, are given at the *top right* of each trace. The lipid bilayer was held at 0 mV. Channels open upward.

channels in the absence of ATP (38): low $P_o$ channels were poorly activated by $Ca^{2+}$, reaching at 32 μM [$Ca^{2+}$] a maximal $P_o$ value of ~0.03; moderate $P_o$ channels reached their maximal $P_o$ values, ~0.4, at this same 32 μM [$Ca^{2+}$] and displayed inhibition at higher [$Ca^{2+}$]; whereas high $P_o$ channels were maximally activated at 32 μM [$Ca^{2+}$] and showed no inhibition when increasing [$Ca^{2+}$] up to 0.5 mM. The addition of ATP increased the $P_o^*$ at all [$Ca^{2+}$] in channels with any one of the three types of $Ca^{2+}$ responses (Figs. 2 and 3). Single RyR channels from brain incorporated in bilayers gated with fast kinetics between the closed and open states, suggestive of the existence of substates, as previously described (8). This behavior was especially apparent in low and moderate $P_o$ channels at [$Ca^{2+}$] ≥10 μM in the absence of ATP.

Figure 3 shows the mean response of the populations of low, moderate, or high $P_o$ single RyR channels to different [$Ca^{2+}$], both in the absence and the presence of ATP. ATP induced an increase of maximal channel activity; it also shifted channel activation to a lower [$Ca^{2+}$] range and broadened the range of maximal activity (Fig. 3). All these ATP-induced modifications were due to changes in both $K_a$ and $K_i$ for $Ca^{2+}$ (Table 1). The effect of ATP was studied both in control channels (Fig. 3) and in channels that, after thimerosal modification, exhibited the same behavior as control channels (Fig. 3). In control channels, the most conspicuous effect of ATP was observed on the low $P_o$ channels, which displayed a 9.8-fold increase in apparent affinity for activation by $Ca^{2+}$ and a 192-fold decrease in the apparent affinity for inhibition by $Ca^{2+}$ (Table 1). This combined effect produced a significant increase ($P < 0.001$) in maximal activity, from $P_o^* = 0.03 \pm 0.00$ in the [$Ca^{2+}$] range of 32–100 μM to $P_o^* = 0.61 \pm 0.03$ between 10 and 100 μM [$Ca^{2+}$] (Fig. 3*A*). In control channels with moderate $P_o$, $K_a$ decreased 10.7-fold, from 27 ± 6 μM to 2.5 ± 0.4 μM ($P < 0.001$; Table 1); in this case, $K_i$ values could not be determined in the presence of ATP because no data were collected at [$Ca^{2+}$] >100 μM (Fig. 3*B*, *right*). As mentioned above, of the 77 single channels studied, only 1 control channel displayed the high $P_o$ behavior; in this channel, the activating effect of ATP was already apparent at the lowest [$Ca^{2+}$] studied (0.1 μM), and maximal activity was attained at [$Ca^{2+}$] >1 μM with no inhibition up to 1 mM [$Ca^{2+}$] (Fig. 3*C*).

Similar effects of ATP as those observed in the corresponding control channels were observed in channels that attained either the moderate or the high $P_o$ response to $Ca^{2+}$ after incubation with thimerosal (Fig. 3, *B* and *C*). Thus, in channels that, after incubation with thimerosal, attained the moderate $P_o$ behavior, ATP induced a 6.5-fold decrease in $K_a$ and a 13.4-fold increase in $K_i$. ATP induced comparable changes in the $Ca^{2+}$ dependence of both control and thimerosal-modified moderate $P_o$ channels. In thimerosal-modified channels that attained the high $P_o$ behavior, $K_a$ increased 8.2-fold (Table 1). The apparent affinities for inhibition by $Ca^{2+}$ were beyond the range of the highest [$Ca^{2+}$] studied and hence could not be determined accurately.

*Inhibition of RyR single-channel activity by $Mg^{2+}$.* Since the [$^3$H]ryanodine binding experiments demonstrated an inhibitory effect of $Mg^{2+}$, we tested the effect of $Mg^{2+}$ on single-channel activity. The effect of $Mg^{2+}$ was determined in the presence of 3 mM free [ATP] and 32 μM free [$Ca^{2+}$]. These concentrations were chosen because, as shown in Fig. 3, *right*, in these conditions, all channels were maximally activated in the absence of $Mg^{2+}$, regardless of their response to $Ca^{2+}$. The effect of $Mg^{2+}$ was tested in control channels with the low or the moderate $P_o$ behavior (Fig. 4). The most significant inhibitory effect of $Mg^{2+}$ was observed in low $P_o$ channels, with a $K_{i\,Mg}$ value of 0.24 ± 0.03 mM (Fig. 4). In moderate $P_o$ channels, the inhibitory effect of $Mg^{2+}$ was less marked than in low $P_o$ channels ($K_{i\,Mg} = 1.1 \pm 0.2$ mM; $P = 0.002$) (Fig. 4). $Mg^{2+}$ inhibition of low $P_o$ channels was cooperative, with a Hill coefficient ($n_H$) of 1.6 ± 0.3, whereas inhibition of moderate $P_o$

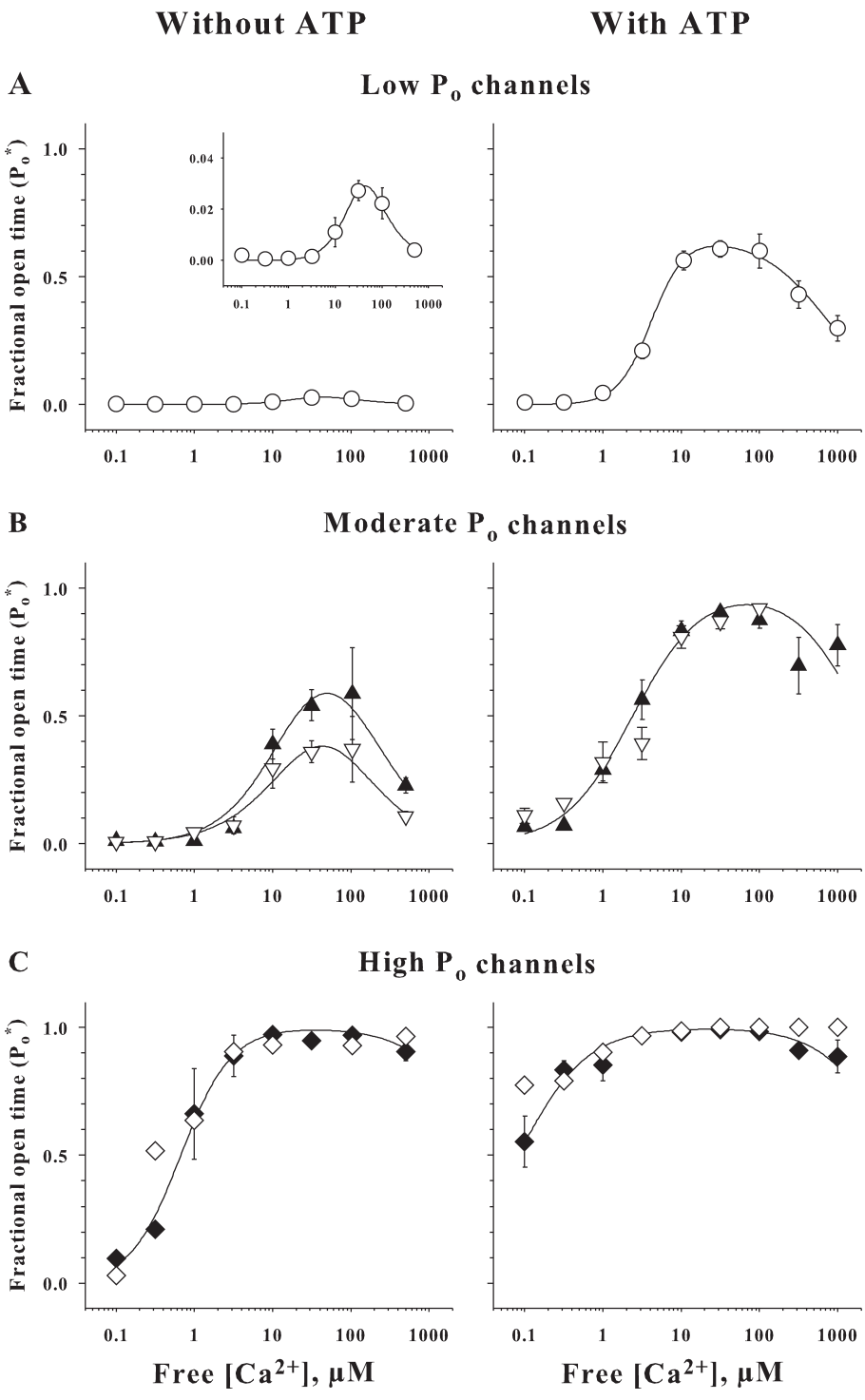


Fig. 3. $Ca^{2+}$ response curves of single low, moderate, and high $P_o$ RyR channels are modified by ATP. Fractional open times ($P_o^*$) of low (circles), moderate (triangles), and high $P_o$ channels (diamonds) are depicted as a function of free [$Ca^{2+}$] in the absence (*left*) or presence (*right*) of 3 mM free [ATP]. *A*, *left*, *inset*: an expansion of the vertical axis of data of low $P_o$ channels obtained in the absence of ATP. Data were obtained with the following number of single-channel experiments: 24 control low $P_o$ channels (open circles); 11 control (open triangles) and 17 thimerosal-modified (solid triangles) moderate $P_o$ channels; and 1 control (open diamonds) and 9 thimerosal-modified (solid diamonds) high $P_o$ channels. Symbols and error bars depict mean and SE values, respectively. Here and in Figs. 4 and 5, the error bar is hidden within the symbol in several cases. Solid lines show the best nonlinear fits to *Eq. 1*, performed with all individual values obtained in each condition studied (see MATERIALS AND METHODS). For moderate $P_o$ channels with ATP and high $P_o$ channels (with or without ATP), the fits correspond to thimerosal-modified channels. All parameter values obtained are displayed in Table 1.

channels was not cooperative ($n_H$ = 1.0 ± 0.3). The effect of $Mg^{2+}$ on control channels with high $P_o$ could not be studied because of the low frequency of incorporation in the bilayer of channels with this behavior.

In channels that, after incubation with thimerosal, attained the moderate $P_o$ behavior, $Mg^{2+}$ induced similar channel inhibition as that observed in control moderate $P_o$ channels (Fig. 4). $K_{i\,Mg}$ did not differ between thimerosal-modified (0.79 ± 0.29 mM) and control moderate $P_o$ channels ($P$ = 0.459). In channels that attained the high $P_o$ behavior after incubation with thimerosal, the inhibitory effect of $Mg^{2+}$ was minimal at [$Mg^{2+}$] up to 1 mM (Fig. 4). The fitted value of $K_{i\,Mg}$ was 9.3 ± 1.6 mM; however, we did not carry out measurements at [$Mg^{2+}$] >1 mM to obtain precise values for $K_{i\,Mg}$ or $n_H$ for high $P_o$ channels.

*$Ca^{2+}$ dependence at near physiological ATP and $Mg^{2+}$ concentrations.* To mimic in our in vitro setting, the presumed intracellular conditions, we investigated the $Ca^{2+}$ dependence

Table 1. *Fitting parameters for control or thimerosal-modified RyR channels with low, moderate, or high $P_o$ behavior at different cytoplasmic [ATP] and [$Mg^{2+}$]*

| | Controls | | | Thimerosal Modified | | |
|---|---|---|---|---|---|---|
| Channel Behavior | [ATP] = 0, [$Mg^{2+}$] = 0 | [ATP] = 3, [$Mg^{2+}$] = 0 | [ATP] = 0.5, [$Mg^{2+}$] = 0.8 | [ATP] = 0, [$Mg^{2+}$] = 0 | [ATP] = 3, [$Mg^{2+}$] = 0 | [ATP] = 0.5, [$Mg^{2+}$] = 0.8 |
| Low $P_o$ | | | | | | |
| $K_a$, μM | 40±9 | 4.1±0.6‡ | 151±22‡ | | | |
| $n_H$ | 2.0±0.4 | 2.1±0.3 | 1.4±0.2 | | | |
| $K_i$, μM | 3.9±1.0 | 751±203‡ | 185±26‡ | | | |
| $P_{o\ max}$ | 0.65* | 0.65±0.03 | 0.65* | | | |
| Moderate $P_o$ | | | | | | |
| $K_a$, μM | 27±6 | 2.5±0.4‡ | 188±35‡ | 16±2† | 2.4±0.3‡ | 197±44‡ |
| $n_H$ | 1.0±0.2† | 1* | 1.1±0.2 | 1.1±0.2† | 1.0±0.1 | 1.3±0.3 |
| $K_i$, μM | 72±19‡ | § | 352±63‡ | 153±27‡ | 2,000* | 1,030±337† |
| $P_{o\ max}$ | 1* | 1* | 1* | 1* | 1* | 1* |
| High $P_o$ | | | | | | |
| $K_a$, μM | 0.46±0.10‡ | 0.04±0.01† | | 0.67±0.09‡ | 0.08±0.01‡ | 14±3‡ |
| $n_H$ | 1.1±0.3 | 1* | | 1.4±0.2 | 1* | 1.1±0.2 |
| $K_i$, μM | 5,500* | 5,500* | | 5,500* | 5,500* | 9,000* |
| $P_{o\ max}$ | 1* | 1* | | 1* | 1* | 1* |

Parameter values ± SE were obtained by fitting all individual data obtained for each experimental condition to *Eq. 1* (see MATERIALS AND METHODS). [ATP] and [$Mg^{2+}$] correspond to free (uncomplexed) ATP and $Mg^{2+}$ concentrations (mM), respectively, present in cytoplasmic compartment. Control channels correspond to channels without incubation with thimerosal. $K_a$ and $K_i$, $Ca^{2+}$ concentrations for half-maximal activation and inhibition, respectively; $n_H$, Hill coefficient; $P_o$, fractional open time; $P_{o\ max}$, maximal $P_o$; RyR, ryanodine receptor. Significant differences (‡$P \leq 0.001$ or †$P < 0.05$) between corresponding parameter values are indicated. Parameter values obtained with ATP or ATP plus $Mg^{2+}$ were compared with those obtained in the absence of ATP. Parameter values of moderate $P_o$ channels (control or thimerosal modified) obtained in the absence of ATP were compared with values of control low $P_o$ channels without ATP. Values of high $P_o$ channels (control or thimerosal modified) obtained in the absence of ATP were compared with the values of control moderate $P_o$ channels without ATP. *Parameter was fixed to the indicated value for data fitting. §Data were fitted to a particular case of *Eq. 1*: $P_o^* = (P_{o\ max} \times [Ca^{2+}]^n)/([Ca^{2+}]^n + K_a^n)$, where $n$ is Hill coefficient for $Ca^{2+}$ activation.

of brain cortex RyR channels at 0.5 mM free [ATP] and 0.8 mM free [$Mg^{2+}$], concentrations reported within the physiological range in brain (60, 64). Figure 5 shows that, in these conditions, the $Ca^{2+}$ dependencies of low, moderate, and high $P_o$ channels were shifted to higher [$Ca^{2+}$] when compared with the $Ca^{2+}$ dependencies measured in the absence of ATP and $Mg^{2+}$ (Fig. 3, *left*). In the presence of these ATP and $Mg^{2+}$ concentrations, maximal channel activity for channels with any one of the three $Ca^{2+}$ responses was attained near 300 μM [$Ca^{2+}$], around 10 times higher than the value of 32 μM observed in the absence of ATP and $Mg^{2+}$ (compare Fig. 5

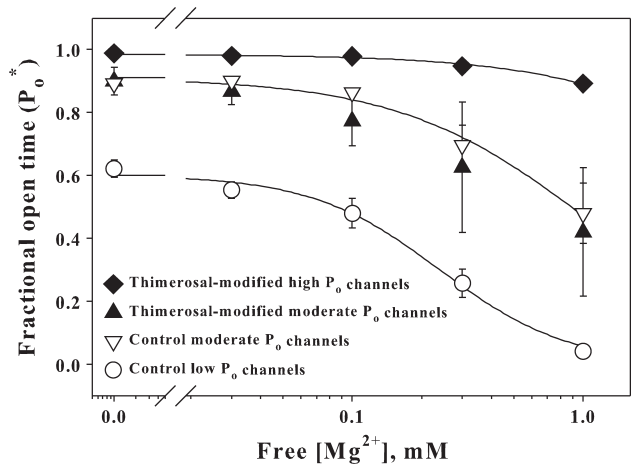


Fig. 4. Inhibition by $Mg^{2+}$ of brain RyR channels displaying the 3 different responses to cytoplasmic [$Ca^{2+}$]. Mean fractional open times ($P_o^*$) are depicted as a function of free [$Mg^{2+}$] in the presence of 3 mM free [ATP] and 32 μM free [$Ca^{2+}$]. Data were obtained with 7 control low (open circles), 4 control moderate (open triangles), 5 thimerosal-modified moderate (solid triangles), and 4 thimerosal-modified high (solid diamonds) $P_o$ channels. Symbols and error bars depict mean and SE values, respectively. Solid lines represent the best nonlinear fits of all individual experimental data values obtained for control channels with low or moderate $P_o$ and for thimerosal-modified high $P_o$ channels to *Eq. 2* (see MATERIALS AND METHODS). Parameter values are given in RESULTS.

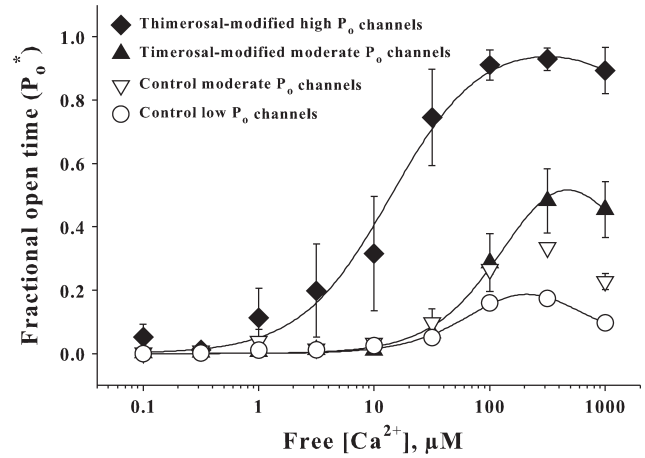


Fig. 5. $Ca^{2+}$ dependencies of low, moderate, and high $P_o$ channels at near physiological concentrations of $Mg^{2+}$ and ATP. Mean fractional open times ($P_o^*$) are depicted as a function of free [$Ca^{2+}$] in the presence 0.8 mM free [$Mg^{2+}$] and 0.5 mM free [ATP]. Data were obtained using control channels with low ($N = 4$, open circles) or moderate ($N = 3$ open triangles) $P_o$ response and thimerosal-modified channels with moderate ($N = 5$, solid triangles) or high $P_o$ behavior ($N = 4$, solid diamonds). Symbols and error bars depict mean and SE values, respectively. Solid lines represent the best nonlinear fits to *Eq. 1* of all individual experimental data values obtained with control low, thimerosal-modified moderate, and thimerosal-modified high $P_o$ single channels (see MATERIALS AND METHODS). All parameter values obtained are displayed in Table 1.

with Fig. 3, *left*). Therefore, the combined effects of ATP stimulation and $Mg^{2+}$ inhibition resulted in a net shift to the right of the $Ca^{2+}$ activation curve. In addition, in these conditions, the activity of low $P_o$ channels increased from an almost negligible maximal value of 0.03 ± 0.00 to a value of 0.17 ± 0.01 ($P < 0.001$); in contrast, moderate and high $P_o$ channels did not vary significantly in their maximal activity ($P > 0.3$). In the $[Ca^{2+}]$ range that is presumably reached during neuronal activity (1–10 μM), only high $P_o$ channels displayed clear activation. At $[Ca^{2+}] > 100$ μM, concentrations that could be reached locally in the immediate vicinity of presynaptic $Ca^{2+}$ entry sites, even low $P_o$ channels, were somewhat activated.

The above experiments at near physiological concentrations of ATP and $Mg^{2+}$ were carried out in control low $P_o$ channels, in control and thimerosal-modified moderate $P_o$ channels, and in thimerosal-modified high $P_o$ channels. A representative experiment, shown in Fig. 6, illustrates the $Ca^{2+}$ response at near physiological concentrations of ATP and $Mg^{2+}$ of a control moderate $P_o$ channel (Fig. 6, *left*) that, after incubation with thimerosal, acquired the high $P_o$ behavior (Fig. 6, *right*). After incubation with thimerosal, the channel showed marked activation by $Ca^{2+}$ in the concentration range from 10 to 32 μM ($P_o^*$ values between 0.25 and 0.94), whereas, before incubation, it responded poorly to these $[Ca^{2+}]$ ($P_o^*$ values <0.15).

The net shift to the right of the $Ca^{2+}$ dependence curves obtained by data fitting to *Eq. 1*, induced by the combined presence of near physiological concentrations of ATP and $Mg^{2+}$, reflects an increase in both $K_a$ and $K_i$ (Table 1). $K_a$ values increased in all channels: 3.7-fold for low $P_o$ channels; 6.9- or 12.6-fold for control or thimerosal-modified moderate $P_o$ channels, respectively; and 21-fold for high $P_o$ channels. The $K_i$ values also increased in all cases, especially in low $P_o$ channels (47-fold), whereas, in thimerosal-modified moderate $P_o$ channels, $K_i$ increased 6.7-fold. Eventual changes in $K_i$ could not be accurately determined in high $P_o$ channels because of the range of $[Ca^{2+}]$ used in our experiments.

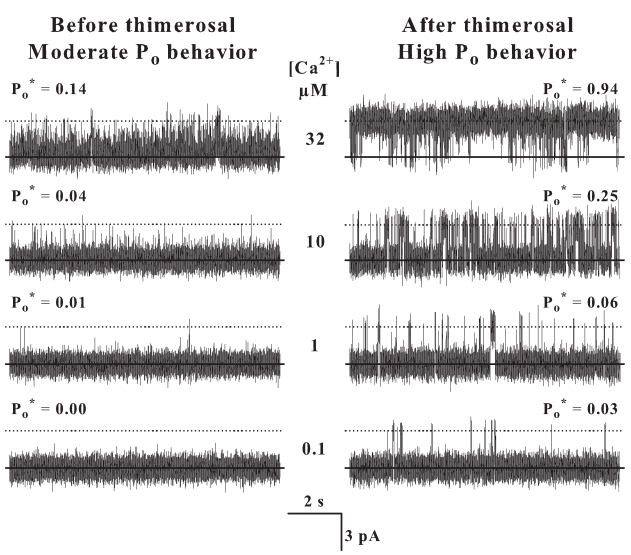


Fig. 6. Thimerosal treatment enhances activation by $Ca^{2+}$ of a single channel at near physiological concentrations of $Mg^{2+}$ and ATP. Representative current recordings were obtained before (*left*) and after incubation with thimerosal (*right*) at the indicated cytoplasmic free $[Ca^{2+}]$ with fixed 0.8 mM free $[Mg^{2+}]$ and 0.5 mM free [ATP]. Average $P_o^*$ values, calculated from at least 120 s of continuous recordings, are given near each trace. The lipid bilayer was held at 0 mV. Channel opens upward.

## DISCUSSION

An increase in cytoplasmic $[Ca^{2+}]$ has the potential to elicit RyR channel activation and thus give rise to RyR-mediated CICR, a process that in cells must occur in the presence of ATP and $Mg^{2+}$. The epitome of the RyR-mediated CICR process is the activation by $Ca^{2+}$ of the RyR2 isoform in cardiac muscle cells, which precedes cardiac muscle contraction during each heartbeat. In brain, CICR is emerging as an amplifying mechanism that participates in important signaling pathways in neurons (5, 12, 23, 26, 61–63). However, the regulation of neuronal RyR channels is presently not well known, and there are few reports regarding the properties and regulation of RyR channels from brain at the single-channel level (2, 8, 34, 38, 39, 43, 55).

*Effect of ATP on the $Ca^{2+}$ dependence of RyR channels.* We found that ATP enhanced RyR channel sensitivity to $Ca^{2+}$ activation, irrespective of $Ca^{2+}$ response, as reflected by the significant decrease in $K_a$ values for $Ca^{2+}$ ~1 order of magnitude in control or thimerosal-modified brain RyR channels. By comparison, AMP-PCP reduces $K_a$ values in cardiac RyR2 only by around one-half (45, 68), while ATP has a minor effect on RyR3 from skeletal muscle at low $[Ca^{2+}]$ (28, 58), albeit opposing results with mink RyR3 expressed in HEK293 cells have been reported (37). We also found that ATP was very effective in decreasing channel inhibition by high $[Ca^{2+}]$, as evidenced by the increase in $K_i$ values in brain RyR, especially in the case of low $P_o$ channels. This particular channel behavior has not been described for RyR2 from heart muscle or for RyR3 from skeletal muscle or brain tissue (14, 16, 28, 36, 47, 49). In the presence of ATP analogs or AMP, RyR3 channels purified from skeletal muscle (47, 48) or brain tissue (49) display $K_i$ values ~3 mM, a value we only found for brain channels with the high $P_o$ behavior, which are presumably oxidized.

Our present results showing that ATP increased the apparent affinity for $Ca^{2+}$ activation and, in addition, decreased the apparent affinity for $Ca^{2+}$ inhibition, are very similar to the changes induced by redox modification. Thus redox modification/alkylation of SH residues increases the apparent affinity for $Ca^{2+}$ activation and decreases the apparent affinity for $Ca^{2+}$ inhibition (see Table 1), whereas reduction to free SH residues has the opposite effects (39). The effect of ATP on RyR channels has been ascribed to ATP binding to an adenine nucleotide site (44), which, via an allosteric change, modifies the affinity of $Ca^{2+}$ binding sites (45). Therefore, by analogy with the effects of ATP, redox modification/alkylation of key cysteines may modify the affinity of the $Ca^{2+}$ binding sites by inducing an allosteric change, presumably through a different mechanism than that proposed for ATP, since the effects of alkylation and ATP seem to be additive.

*Inhibition of RyR channel activity by $Mg^{2+}$.* We report here novel findings regarding redox effects on the inhibition of brain RyR by $Mg^{2+}$. Equilibrium [$^3$H]ryanodine binding density is commonly reported in the literature as a means by which to assess the activity of RyR channel populations, since ryanodine binds to active (open) channels. As previously reported for brain RyR (42, 51, 57, 69), $Mg^{2+}$ inhibited [$^3$H]ryanodine

binding to brain cortex ER vesicles. Yet, the $K_{i\,Mg}$ value found in this work for control vesicles is lower by an order of magnitude than the $K_{i\,Mg} \geq 5$ mM reported in the literature for vesicles obtained from rat brain cortex (51, 69) or for RyR purified from whole rabbit brain (42). Furthermore, the $K_{i\,Mg}$ values varied significantly after modifying the redox state of the receptors with DTT or thimerosal, strongly suggesting that SH residues somehow control the affinity of the $Mg^{2+}$ binding site. Thus $K_{i\,Mg}$ values decreased from 0.85 to 0.48 mM after incubation with DTT, while, after incubation with thimerosal, $K_{i\,Mg}$ increased from 0.85 to 2.9 mM, a value comparable to those reported previously for brain RyR (42, 51, 69). We routinely included DTT in all steps of the procedure used to isolate ER vesicles to prevent oxidation of SH residues. In contrast, vesicles used in previous reports were isolated without DTT or other SH reducing agents (42, 51, 69), raising the possibility that critical RyR SH residues were oxidized during membrane isolation, originating the reported high $K_{i\,Mg}$ values (42, 51, 69). Our single-channel measurements are consistent with this idea, since channels that, after incubation with thimerosal, attained the high $P_o$ behavior were poorly inhibited by $Mg^{2+}$, showing a $K_{i\,Mg} > 5$ mM. This value is similar to the $K_{i\,Mg}$ obtained for [$^3$H]ryanodine binding experiments to vesicles incubated with thimerosal and to values reported in the literature for [$^3$H]ryanodine binding experiments (42, 51, 69).

In contrast, control low $P_o$ channels displayed the lowest $K_{i\,Mg}$ value (0.24 mM). This value is in the same order of magnitude as that obtained in our binding experiments in the presence of DDT (0.48 mM), strongly suggesting that control low $P_o$ channels had the greater fraction of critical SH residues in the reduced state.

The $K_{i\,Mg}$ values of control (1.1 mM) and thimerosal-modified (0.79 mM) moderate $P_o$ single channels were comparable with the value obtained when measuring [$^3$H]ryanodine binding in control vesicles in the absence of DTT (0.85 mM). This similarity suggests that, during the long incubation period required to measure [$^3$H]ryanodine binding at equilibrium (120 min at 37°C), channels attained the moderate $P_o$ state because the initial concentration of DTT present in the vesicle preparation was diluted to ~0.15 mM during binding, a value presumably too low to keep most channels in the reduced state.

Low $P_o$ channels, which represent 77% of all RyR channels incorporated in the bilayers, were inhibited by $Mg^{2+}$ at submillimolar concentrations when measured in the presence of activating concentrations of ATP (3 mM) and $Ca^{2+}$ (32 μM). In our study, only the extremely infrequent high $P_o$ channels displayed $K_{i\,Mg}$ values comparable to those reported for cardiac RyR2 and skeletal RyR3 channels (47, 65) ($K_{i\,Mg} > 2$ mM).

The inhibitory effect of $Mg^{2+}$ on RyR might result from competition with $Ca^{2+}$ at the $Ca^{2+}$ activating cytoplasmic site or from $Mg^{2+}$ binding to the divalent inhibitory site (35). Since we tested $Mg^{2+}$ inhibition at activating concentrations of ATP (or AMP-PNP) and at [$Ca^{2+}$] high enough to saturate the $Ca^{2+}$ activating site, in our experimental conditions, $Mg^{2+}$ is likely to bind preferentially to the divalent inhibitory site.

On the basis of the present results, which show that thimerosal decreases $Mg^{2+}$ inhibition while the reducing agent DTT increases it, we propose that the redox state of a few highly reactive RyR cysteine residues determines the apparent affinity of $Mg^{2+}$ for the divalent inhibitory site; according to this view, alkylation of these key RyR cysteines decreases the apparent affinity of $Mg^{2+}$, while their reduction increases it. A similar model was previously proposed for the skeletal RyR1 isoform (1).

*$Ca^{2+}$ dependence at near physiological concentrations of $Mg^{2+}$ and ATP.* Under physiological conditions, RyR channels are immersed in an environment containing ATP and $Mg^{2+}$. Therefore, to mimic the intracellular conditions, we measured their $Ca^{2+}$ dependence in the presence of 0.5 mM free [ATP] (total ATP ≥5 mM) plus 0.8 mM free [$Mg^{2+}$], the concentrations presumably present in neurons (60, 64). Addition of $Mg^{2+}$ plus ATP induced a dramatic change in the $Ca^{2+}$ response of the three rat brain channel behaviors, causing a significant increase in $K_a$ and $K_i$ for $Ca^{2+}$ irrespective of their initial $Ca^{2+}$ response. At physiological concentrations of $Mg^{2+}$ and ATP brain RyR channels with low or moderate $P_o$ behaviors were almost inactive up to 10 μM [$Ca^{2+}$]; only high $P_o$ channels showed activation. Moreover, in a single control channel that displayed the moderate $P_o$ behavior, we found that, after incubation with thimerosal, the channel acquired the high $P_o$ behavior so that even low [$Ca^{2+}$] (0.1–32 μM) significantly increased its activity, as shown in Fig. 6.

In summary, RyR channels present in brain cortex ER that should correspond to RyR2 and/or RyR3 (24, 49) behave differently in their response to $Ca^{2+}$ (38, 39) and ATP (8) from RyR2 and RyR3 channels expressed in other tissues and, as shown here, in their response to $Mg^{2+}$ as well. This different behavior of brain cortex RyR channels could result from the presence in vivo of more reduced RyR channels in brain and more oxidized RyR channels in heart and skeletal muscle. Alternatively, it could arise from a differential association of regulatory proteins in their respective macromolecular complexes or from an alternative splicing of their genes in the different tissues. However, these possibilities require further investigation.

Moreover, their calcium dependence changes dramatically with ATP or with physiological concentrations of ATP plus $Mg^{2+}$. Only high $P_o$ channels, presumably more oxidized, respond to moderate increases in [$Ca^{2+}$] in these conditions. The importance of these findings resides in the fact that, to participate in CICR, brain RyR channels must readily increase their activity in response to a cytoplasmic [$Ca^{2+}$] increase. Our results suggest that CICR will be much more efficient in brain cells that have oxidized (high $P_o$) RyR channels than in cells containing less oxidized (moderate $P_o$) channels, which will require a rather dramatic increase in cytoplasmic [$Ca^{2+}$] to engage in CICR. Furthermore, highly reduced (low $P_o$) RyR channels are bound to respond so poorly to $Ca^{2+}$ that brain cells containing this type of channel will probably display negligible CICR. Similarly, redox-dependent changes in CICR could occur in neurons that change their redox conditions (15, 31, 59, 66).

*Cellular implications.* A role for RyR channels as cellular redox sensors has been proposed (20, 27, 53). Activation/inhibition of RyR-mediated CICR by cellular redox species or changes in cellular redox state may represent a physiological mechanism of cross talk between $Ca^{2+}$ and redox signaling pathways (25). Thus we propose that neurons use RyR redox modulation as an additional mechanism to either amplify or inhibit CICR signals as needed for specific physiological responses. An implicit dangerous feature of this proposed mechanism is that oxidative stress may cause excessive CICR,

leading to alterations in $Ca^{2+}$ homeostasis that could produce neuronal excitotoxicity or apoptosis and induce neurodegenerative disorders (40, 41). In particular, RyR channels may be involved in the pathophysiology of neurodegeneration in Alzheimer's disease (13, 30, 46). Conversely, it can be speculated that changes in neuronal redox potential toward increased reduction would shut down the CICR response. Thus, to avoid the detrimental consequences of a redox imbalance, neurons should maintain a delicate redox equilibrium to keep activation of CICR within physiological limits.


## ACKNOWLEDGMENTS

Part of this work was published in abstract form (6, 7).

## GRANTS

This work was supported by FONDAP Grant No. 15010006 and Fondo Nacional de Desarrollo Científico y Tecnológico (FONDECYT) Grant No. 1040717.


## REFERENCES


1. **Aracena P, Sánchez G, Donoso P, Hamilton SL, Hidalgo C.** S-glutathionylation decreases $Mg^{2+}$ inhibition and S-nitrosylation enhances $Ca^{2+}$ activation of RyR1 channels. *J Biol Chem* 278: 42927–42935, 2003.
2. **Ashley RH.** Activation and conductance properties of ryanodine-sensitive calcium channels from brain microsomal membranes incorporated into planar lipid bilayers. *J Membr Biol* 111: 179–189, 1989.
3. **Berridge MJ.** Neuronal calcium signaling. *Neuron* 21: 13–26, 1998.
4. **Berridge MJ, Lipp P, Bootman MD.** The versatility and universality of calcium signalling. *Nat Rev Mol Cell Biol* 1: 11–21, 2000.
5. **Bouchard R, Pattarini R, Geiger JD.** Presence and functional significance of presynaptic ryanodine receptors. *Prog Neurobiol* 69: 391–418, 2003.
6. **Bull R, Finkelstein JP, Maass R, Behrens MI, Hidalgo C.** Regulation of single RyR channels from brain by endogenous modulators (Abstract). *Placenta* 27: A36, 2006.
7. **Bull R, Finkelstein JP, Maass R, Behrens MI, Hidalgo C.** Regulation of RyR channels from rat brain cortex by endogenous modulators (Abstract). *Biophys J* 90: 2006. [The data are available at http://www.biophysics.org/abstracts/]
8. **Bull R, Marengo JJ, Finkelstein JP, Behrens MI, Alvarez O.** SH oxidation coordinates subunits of rat brain ryanodine receptor channels activated by calcium and ATP. *Am J Physiol Cell Physiol* 285: C119–C128, 2003.
9. **Bull R, Marengo JJ, Suárez-Isla BA, Donoso P, Sutko JL, Hidalgo C.** Activation of calcium channels in sarcoplasmic reticulum from frog muscle by nanomolar concentrations of ryanodine. *Biophys J* 56: 749–756, 1989.
10. **Carafoli E.** Calcium signaling: a tale for all seasons. *Proc Natl Acad Sci USA* 99: 1115–1122, 2002.
11. **Carrasco MA, Jaimovich E, Kemmerling U, Hidalgo C.** Signal transduction and gene expression regulated by calcium release from internal stores in excitable cells. *Biol Res* 37: 701–712, 2004.
12. **Chameau P, Van de Vrede Y, Dossier P, Baux G.** Ryanodine-, IP3- and NAADP-dependent calcium stores control acetylcholine release. *Pflügers Arch* 443: 289–296, 2001.
13. **Chan SL, Mayne M, Holden CP, Geiger JD, Mattson MP.** Presenilin-1 mutations increase levels of ryanodine receptors and calcium release in PC12 cells and cortical neurons. *J Biol Chem* 275: 18195–18200, 2000.
14. **Chu A, Fill M, Stefani E, Entmann ML.** Cytoplasmic $Ca^{2+}$ does not inhibit the cardiac muscle sarcoplasmic reticulum ryanodine receptor $Ca^{2+}$ channel, although $Ca^{2+}$-induced $Ca^{2+}$ inactivation of $Ca^{2+}$ release is observed in native vesicles. *J Membr Biol* 135: 49–59, 1993.
15. **Crack PJ, Taylor JM.** Reactive oxygen species and the modulation of stroke. *Free Radic Biol Med* 38: 1433–1444, 2005.
16. **Copello JA, Barg S, Onoue H, Fleischer S.** Heterogeneity of $Ca^{2+}$ gating of skeletal muscle and cardiac ryanodine receptors. *Biophys J* 73: 141–156, 1997.
17. **Coronado R, Morrissette J, Sukhareva M, Vaughan DN.** Structure and function of ryanodine receptors. *Am J Physiol Cell Physiol* 266: C1485–C1504, 1994.
18. **De Crescenzo V, Fogarty KE, Zhuge R, Tuft RA, Lifshitz LM, Carmichael J, Bellvé KD, Baker SP, Zissimopoulos S, Lai FA, Lemos JR, Walsh JV Jr.** Dihydropyridine receptors and type 1 ryanodine receptors constitute the molecular machinery for voltage-induced $Ca^{2+}$ release in nerve terminals. *J Neurosci* 26: 7565–7574, 2006.
19. **Emptage N, Bliss TV, Fine A.** Single synaptic events evoke NMDA receptor-mediated release of calcium from internal stores in hippocampal dendritic spines. *Neuron* 22: 115–124, 1999.
20. **Eu JP, Sun J, Xu L, Stamler JS, Meissner G.** The skeletal muscle calcium release channel: coupled $O_2$ sensor and NO signaling functions. *Cell* 102: 499–509, 2000.
21. **Furuichi T, Khoda K, Miyawaki A, Mikoshiba K.** Intracellular channels. *Curr Opin Neurobiol* 4: 294–303, 1994.
22. **Futatsugi A, Kato K, Ogura H, Li ST, Nagata E, Kuwajima G, Tanaka K, Itohara S, Mikoshiba K.** Facilitation of NMDAR-independent LTP and spatial learning in mutant mice lacking ryanodine receptor type 3. *Neuron* 24: 701–713, 1999.
23. **Gafni J, Wong PW, Pessah IN.** Non-coplanar 2,2′,3,5′,6 pentachloro biphenyl (PCB 95) amplifies ionotropic glutamate receptor signaling in embryonic cerebellar granule neurons by a mechanism involving ryanodine receptors. *Toxicol Sci* 77: 72–82, 2004.
24. **Giannini G, Conti A, Mammarella S, Scrobogna M, Sorrentino V.** The ryanodine receptor/calcium channel genes are widely and differentially expressed in murine brain and peripheral tissues. *J Cell Biol* 128: 893–904, 1995.
25. **Hidalgo C.** Cross talk between $Ca^{2+}$ and redox signalling cascades in muscle and neurons through the combined activation of ryanodine receptors/$Ca^{2+}$ release channels. *Philos Trans R Soc Lond B Biol Sci* 360: 2237–2246, 2005.
26. **Hidalgo C, Bull R, Behrens MI, Donoso P.** Redox regulation of RyR-mediated $Ca^{2+}$ release in muscle and neurons. *Biol Res* 37: 539–552, 2004.
27. **Hidalgo C, Donoso P, Carrasco MA.** The ryanodine receptors $Ca^{2+}$ release channels: cellular redox sensors? *IUBMB Life* 57: 315–322, 2005.
28. **Jeyakumar LH, Copello JA, O'Malley AM, Wu GM, Grassucci R, Wagenknecht T, Fleischer S.** Purification and characterization of ryanodine receptor 3 from mammalian tissue. *J Biol Chem* 273: 16011–16020, 1998.
29. **Kasai M.** A comment on the analysis of bell-shaped dose-response curves. *Jpn J Physiol* 48: 91–93, 1998.
30. **Kelliher M, Fastbom J, Cowburn RF, Bonkale W, Ohm TG, Ravid R, Sorrentino V, O'Neill C.** Alterations in the ryanodine receptor calcium release channel correlate with Alzheimer's disease neurofibrillary and β-amyloid pathologies. *Neuroscience* 92: 499–513, 1999.
31. **Kemmerling U, Muñoz P, Muller M, Sánchez G, Aylwin ML, Klann E, Carrasco MA, Hidalgo C.** Calcium release by ryanodine receptors mediates hydrogen peroxide-induced activation of ERK and CREB phosphorylation in N2a cells and hippocampal neurons. *Cell Calcium* 41: 491–502, 2007.
32. **Kovalchuk Y, Eilers J, Lisman J, Konnerth A.** NMDA receptor-mediated subthreshold $Ca^{2+}$ signals in spines of hippocampal neurons. *J Neurosci* 20: 1791–1799, 2000.
33. **Kuwajima G, Futatsugi A, Niinobe M, Nakanishi S, Mikoshiba K.** Two types of ryanodine receptors in mouse brain: skeletal muscle type exclusively in Purkinje cells and cardiac muscle type in various neurons. *Neuron* 9: 1133–1142, 1992.
34. **Lai FA, Dent M, Wickenden C, Xu L, Kumari G, Misra M, Lee HB, Sar M, Meissner G.** Expression of a cardiac $Ca^{2+}$-release channel isoform in mammalian brain. *Biochem J* 288: 553–564, 1992.
35. **Laver DR, Baynes TM, Dulhunty AF.** Magnesium inhibition of ryanodine-receptor calcium channels: evidence for two independent mechanisms. *J Membr Biol* 156: 213–229, 1997.
36. **Laver DR, Roden LD, Ahern GP, Eager KR, Junankar PR, Dulhunty AF.** Cytoplasmic $Ca^{2+}$ inhibits the ryanodine receptor from cardiac muscle. *J Membr Biol* 147: 7–22, 1995.
37. **Manunta M, Rossi D, Simeoni I, Butelli E, Romanin C, Sorrentino V, Schindler H.** ATP-induced activation of expressed RyR3 at low free calcium. *FEBS Lett* 471: 256–260, 2000.
38. **Marengo JJ, Bull R, Hidalgo C.** Calcium dependence of ryanodine-sensitive calcium channels from brain cortex endoplasmic reticulum. *FEBS Lett* 383: 59–62, 1996.
39. **Marengo JJ, Hidalgo C, Bull R.** Sulfhydryl oxidation modifies the calcium dependence of ryanodine-sensitive calcium channels. *Biophys J* 74: 1263–1277, 1998.

40. **Mattson MP.** Apoptosis in neurodegenerative disorders. *Nat Rev Mol Cell Biol* 1: 120–129, 2000.
41. **Mattson MP, Chan SL.** Neuronal and glial calcium signaling in Alzheimer's disease. *Cell Calcium* 34: 385–397, 2003.
42. **McPherson PS, Campbell KP.** Characterization of the major brain form of the ryanodine receptor/$Ca^{2+}$ release channel. *J Biol Chem* 268: 19785–19790, 1993.
43. **McPherson PS, Kim YK, Valdivia H, Knudson CM, Takekura H, Franzini-Armstrong C, Coronado R, Campbell KP.** The brain ryanodine receptor: a caffeine-sensitive calcium release channel. *Neuron* 7: 17–25, 1991.
44. **Meissner G.** Ryanodine receptor/$Ca^{2+}$ release channels and their regulation by endogenous effectors. *Annu Rev Physiol* 56: 485–508, 1994.
45. **Meissner G, Henderson JS.** Rapid calcium release from cardiac sarcoplasmic reticulum vesicles is dependent on $Ca^{2+}$ and is modulated by $Mg^{2+}$, adenine nucleotide, and calmodulin. *J Biol Chem* 262: 3065–3073, 1987.
46. **Mungarro-Menchaca X, Ferrera P, Moran J, Arias C.** β-Amyloid peptide induces ultrastructural changes in synaptosomes and potentiates mitochondrial dysfunction in the presence of ryanodine. *J Neurosci Res* 68: 89–96, 2002.
47. **Murayama T, Oba T, Katayama E, Oyamada H, Oguchi K, Kobayashi M, Otsuka K, Ogawa Y.** Further characterization of the type 3 ryanodine receptor (RyR3) purified from rabbit diaphragm. *J Biol Chem* 274: 17297–17308, 1999.
48. **Murayama T, Ogawa Y.** Characterization of type 3 ryanodine receptor (RyR3) of sarcoplasmic reticulum from rabbit skeletal muscles. *J Biol Chem* 272: 24030–24037, 1997.
49. **Murayama T, Ogawa Y.** Properties of RyR3 ryanodine receptor isoform in mammalian brain. *J Biol Chem* 271: 5079–5084, 1996.
50. **Ouardouz M, Nikolaeva MA, Coderre E, Zamponi GW, McRory JE, Trapp BD, Yin X, Wang W, Woulfe J, Stys PK.** Depolarization-induced $Ca^{2+}$ release in ischemic spinal cord white matter involves L-type $Ca^{2+}$ channel activation of ryanodine receptors. *Neuron* 40: 53–63, 2003.
51. **Padua RA, Nagy JI, Geiger JD.** Ionic strength dependence of calcium, adenine nucleotide, magnesium, and caffeine actions on ryanodine receptors in rat brain. *J Neurochem* 62: 2340–2348, 1994.
52. **Pape HC, Munsch T, Budde T.** Novel vistas of calcium-mediated signalling in the thalamus. *Pflügers Arch* 448: 131–138, 2004.
53. **Pessah IN, Kim KH, Feng W.** Redox sensing properties of the ryanodine receptor complex. *Front Biosci* 7: a72–a79, 2002.
54. **Rousseau E, Smith JS, Henderson JS, Meissner G.** Single channel and $^{45}Ca^{2+}$ flux measurements of the cardiac sarcoplasmic reticulum calcium channel. *Biophys J* 50: 1009–1014, 1986.
55. **Sierralta J, Fill M, Suárez-Isla BA.** Functionally heterogenous ryanodine receptors in avian cerebellum. *J Biol Chem* 271: 17028–17034, 1996.
56. **Simpson PB, Challiss RA, Nahorski SR.** Neuronal $Ca^{2+}$ stores: activation and function. *Trends Neurosci* 18: 299–306, 1995.
57. **Smith SM, Nahorski SR.** Characterisation and distribution of inositol polyphosphate and ryanodine receptors in the rat brain. *J Neurochem* 60: 1605–1614, 1993.
58. **Sonnleitner A, Conti A, Bertocchini F, Schindler H, Sorrentino V.** Functional properties of the ryanodine receptor type 3 (RyR3) $Ca^{2+}$ release channel. *EMBO J* 17: 2790–2798, 1998.
59. **Sultana R, Boyd-Kimball D, Poon HF, Cai J, Pierce WM, Klein JB, Markesbery WR, Zhou XZ, Lu KP, Butterfield DA.** Oxidative modification and down-regulation of Pin1 in Alzheimer's disease hippocampus: a redox proteomics analysis. *Neurobiol Aging* 27: 918–925, 2006.
60. **Taylor JS, Vigneron DB, Murphy-Boesch J, Nelson SJ, Kessler HB, Coia L, Curran W, Brown TR.** Free magnesium levels in normal human brain and brain tumors: $^{31}P$ chemical-shift imaging measurements at 1.5 T. *Proc Natl Acad Sci USA* 88: 6810–6814, 1991.
61. **Verkhratsky A.** The endoplasmic reticulum and neuronal calcium signaling. *Cell Calcium* 32: 393–404, 2002.
62. **Verkhratsky A.** Physiology and pathophysiology of the calcium store in the endoplasmic reticulum of neurons. *Physiol Rev* 85: 201–279, 2005.
63. **Verkhratsky A, Petersen OH.** The endoplasmic reticulum as an integrating signalling organelle: from neuronal signalling to neuronal death. *Eur J Pharmacol* 447: 141–154, 2002.
64. **Vink R, McIntosh TK, Demediuk P, Weiner MW, Faden AI.** Decline in intracellular free $Mg^{2+}$ is associated with irreversible tissue injury after brain trauma. *J Biol Chem* 263: 757–761, 1988.
65. **Xu L, Mann G, Meissner G.** Regulation of cardiac $Ca^{2+}$ release channel (ryanodine receptor) by $Ca^{2+}$, $H^+$, $Mg^{2+}$, and adenine nucleotides under normal and simulated ischemic conditions. *Circ Res* 79: 1100–1109, 1996.
66. **Yermolaieva O, Brot N, Weissbach H, Heinemann SH, Hoshi T.** Reactive oxygen species and nitric oxide mediate plasticity of neuronal calcium signaling. *Proc Natl Acad Sci USA* 97: 448–453, 2000.
67. **Yount RG, Babcock D, Ballantyne W, Ojala D.** Adenylyl imidodiphosphate, an adenosine triphosphate analog containing a P-N-P linkage. *Biochemistry* 22: 2484–2489, 1971.
68. **Zimanyi I, Pessah IN.** Comparison of [$^3$H]ryanodine receptors and $Ca^{++}$ release from rat cardiac and rabbit skeletal muscle sarcoplasmic reticulum. *J Pharmacol Exp Ther* 256: 938–946, 1991.
69. **Zimanyi I, Pessah IN.** Pharmacological characterization of the specific binding of [$^3$H]ryanodine to rat brain microsomal membranes. *Brain Res* 561: 181–191, 1991.
70. **Zucchi R, Ronca-Testoni S.** The sarcoplasmic reticulum $Ca^{2+}$ channel/ryanodine receptor: modulation by endogenous effectors, drugs and disease states. *Pharmacol Rev* 49: 1–51, 1997.